International Journal of Creative and Open Research in Engineering and Management
ISSN: **3108-1754 (Online)**
Volume 02 Issue 04 April-2026 | Impact Factor: 3.5

Intelligent Fault Diagnosis of Rolling Element Bearings using Finite Element Analysis

Pratiksha Jadhav

TE Mechanical Engineering

Guide :- **Patil Mangesh** Sir (Assistant Professor)

Department Of Mechanical Engineering, In Adsul's Technical Campus Chas Ahillyanagar 414005, India

How to Cite this Article:

Jadhav, P. (2026). Intelligent Fault Diagnosis of Rolling Element Bearings using Finite Element Analysis. International Journal of Creative and Open Research in Engineering and Management, 02(04). https://doi.org/10.55041/ijcope.v2i4.501

https://doi.org/10.55041/ijcope.v2i4.501

Abstract: Rolling element bearings play a vital role in rotating machines such as motors, pumps, turbines, and gearboxes. Any malfunction in these components can cause sudden equipment failure, unplanned downtime, loss of production, and increased repair expenses. Therefore, timely and reliable fault detection is necessary to maintain operational safety and enhance system dependability. This study proposes an intelligent fault diagnosis method for rolling element bearings based on transient Finite Element Analysis (FEA). A transient FEA model is constructed to capture the time-dependent dynamic behavior of the bearing under varying loads, rotational speeds, and defect conditions. The model allows detailed investigation of parameters such as stress distribution, deformation, contact interactions, and vibration characteristics throughout the operating cycle. Different fault types, including defects in the inner race, outer race, and rolling elements, are introduced into the simulation to obtain distinctive dynamic patterns that assist In accurate fault identification. The dynamic responses obtained from the simulations are further analyzed using advanced signal processing methods and intelligent computational techniques. Relevant features are extracted from the time-domain and frequency-domain signals and supplied to machine learning models for automatic identification of fault categories and their severity levels. This approach achieves reliable diagnostic performance while minimizing the need for extensive experimental testing and physical trials. In addition, it supports predictive maintenance by enabling early detection of potential defects before serious damage occurs. The findings confirm that the integration of transient Finite Element Analysis with intelligent data-driven analysis forms a robust and efficient framework for condition monitoring and timely fault diagnosis of rolling element bearings in industrial environments.

Keywords: Tapered rolling bearing defect; Time-domain; Frequency-domain; Vibration; Conditioning monitoring

1. Introduction: Rolling element bearings primary purpose is to carry mechanical loads, minimize friction between moving parts, and provide stable and smooth rotational motion. However, these bearings are exposed to varying loads, high rotational speeds, and challenging environmental conditions such as temperature fluctuations, contamination, and inadequate lubrication. Due to these demanding conditions, bearings are prone to different types of defects, including damage to the inner race, outer race, rolling elements, misalignment, and lubrication- related issues. The presence of such defects can cause abnormal vibrations, increased noise levels, reduced efficiency, and progressive deterioration of machine performance, which may eventually result in unexpected breakdowns or complete system failure. Consequently, implementing reliable and timely fault detection techniques for rolling element bearings is crucial for improving operational safety, reducing maintenance expenses, preventing unplanned shutdowns, and ensuring the overall dependability of industrial machinery. Traditional fault diagnosis techniques primarily depend on vibration monitoring, signal analysis, and experimental investigations to detect bearing defects. While these methods can provide valuable insights into machine condition, they often require extensive experimental data and significant human intervention. In addition, they may fail to accurately represent the internal stress patterns and transient dynamic responses of bearings during actual operating conditions. Experimental procedures are also generally time-consuming, expensive, and difficult to implement for evaluating multiple fault types or varying operating scenarios. As a result, relying solely on conventional approaches can limit diagnostic accuracy and efficiency. To address these challenges, Finite Element Analysis (FEA) has become a powerful computational approach for studying the behavior of rolling element bearings. This technique allows precise modeling and simulation of bearing components, enabling detailed evaluation of stress distribution, strain, deformation, and contact interactions under different loading and boundary conditions. In particular, transient FEA is highly effective for analyzing time-varying dynamic responses, including impact loads, vibration patterns, and fluctuating stresses generated when defects move through the load- carrying zone. Such time-domain simulations closely represent real operating environments and facilitate the identification of fault-related dynamic features with greater accuracy and reliability.

By combining transient FEA simulations with intelligent fault diagnosis methods such as signal processing, machine learning, and pattern recognition, automated detection and classification of bearing defects can be achieved with high precision. The transient responses generated through simulation provide consistent and reliable datasets for training intelligent models, thereby minimizing the reliance on large- scale experimental measurements. This integrated strategy enhances diagnostic accuracy, enables early fault prediction, and facilitates the implementation of predictive maintenance practices. Consequently, it contributes to improved reliability, reduced downtime, and more effective overall machinery health management. Therefore, the use of intelligent fault diagnosis combined with transient Finite Element Analysis (FEA) offers a robust and economical framework for analyzing bearing dynamic behavior, identifying early-stage defects, and maintaining the safe and dependable operation of industrial rotating machinery.

Fig 1: Fault detection in taper bearing

Table 1. Literature review

Author & Year	Bearing Type	Defect Type	Defect On	Speed (RPM)	Load (N/HP)	Unbalance	Feature Extraction	Response	Method
Iunusova et al. (2024) (Springer)	Deep groove ball bearing	Early-stage fault	Inner/Outer race	1000–1500	0–3 HP	Not considered	Frequency domain	Clear defect bands	Knowledge-based + Data- driven
Zheng et al. (2024) (Nature)	Rolling element bearing	Impact fault	Rolling element	1200–1800	Variable	Yes	Nonlinear dynamic features	High impulse response	Nonlinear FEA + vibration
Chen et al. (2024) (Nature)	Ball bearing	Localized defect	Inner race	1500	500–1000 N	No	Statistical features	Improved accuracy	GA + BP Neural Network
Fang et al. (2023) (MDPI)	Rolling bearing	Multi-fault	Inner + Outer race	1000–1500	Medium	Yes	Feature fusion	Enhanced sensitivity	Signal fusion + fuzzy logic
Sahu et al. (2025) (Springer)	Ball bearing	Operational fault	All components	500–1500	Variable	Yes	Deep features	High classification accuracy	CNN-LSTM
Patel & Patel (2023) (Sage Journals)	Rolling element bearing	General faults	All	Variable	Variable	Yes	Time-frequency features	Robust detection	Signal processing techniques
JSV Model Study (2023) (ScienceDirect)	Rolling bearing	Rolling element defect	Ball	900–1500	0–30 N	Yes	Time-domain + FFT	Fault frequency amplification	Dynamic modeling + FEA
Pubalan et al. (2026) (arXiv)	Ball bearing	Inner/Outer/ Ball	All	0–1800	0–3 HP	Yes	Raw signal (automatic)	~99% accuracy	1D CNN
Al-Sa'd et al. (2024) (arXiv)	Rolling bearing	Non-stationary fault	All	Variable	Variable	Yes	Time-frequency distribution	Noise-robust	TF-CNN
Jalonen et al. (2023) (arXiv)	Rolling bearing	Multiple faults	Inner/Outer /Ball	Variable	Variable	Yes	Spectral separability	Real- time response	CNN + SSA

Recent research on intelligent fault diagnosis of rolling element bearings highlights a clear shift toward combining vibration signal analysis, artificial intelligence, and physics-based modeling to enhance diagnostic performance and enable early fault detection. For instance, studies by Iunusova et al. (2023–2024) emphasize the use of vibration signatures through both knowledge-driven and data-driven methods, demonstrating that frequency- domain features play a crucial role in identifying early-stage defects. In a similar direction, Sahu et al. (2024– 2025) proposed a hybrid deep learning framework integrating convolutional neural networks (CNN) and long short-term memory (LSTM) networks, supported by empirical mode decomposition (EMD) for feature extraction. Their approach achieved very high accuracy in detecting wear-related faults under varying operational conditions. Complementing these data-driven methods, Zheng et al. (2024) developed a nonlinear dynamic model based on impact interactions, offering insights into fault progression influenced by load and speed variations, with concepts closely aligned to finite element modeling. Other researchers have explored optimization-based techniques. Chen et al. (2024), for example, combined genetic algorithms with neural networks to enhance prediction accuracy by optimizing model parameters. Review studies such as those by Patel and Patel (2023) and Kannan et al. (2024) consistently highlight the growing importance of advanced signal processing and intelligent feature extraction in improving diagnostic reliability. Handling non-stationary vibration signals remains a key challenge, and Pandiyan et al. (2024) demonstrated that EMD-based techniques are particularly effective in this context. More advanced approaches, including deep convolutional fuzzy systems and entropy-based methods using SSA-VMD, have been shown to improve robustness against noise and enhance feature representation. Most recently, deep learning models that operate directly on raw vibration signals, as presented by Pubalan et al. (2026), have shown strong potential for real-time applications. These models eliminate the need for extensive manual feature engineering while maintaining high diagnostic accuracy across different working conditions. The integration of physics-based modeling, advanced signal processing, and artificial intelligence forms a comprehensive and effective framework for accurate, reliable, and early fault diagnosis in rolling element bearings.

2. Methodology: This study presents an intelligent framework for diagnosing faults in rolling element bearings by combining finite element modeling with data-driven analysis. The process begins with the creation of a detailed finite element model of the bearing system, including key components such as the inner race, outer race, rolling elements, and cage. Appropriate material properties, contact conditions, and boundary constraints are defined to closely mimic real operating environments. Simulations are then carried out under different loading and operational conditions to analyze the dynamic response of the bearing. To represent fault conditions, defects are intentionally introduced into specific components, such as localized damage on the inner race, outer race, or rolling elements, allowing the generation of corresponding vibration signals.

The vibration data obtained from these simulations are further processed to reveal important fault-related characteristics. Since bearing signals are typically non-stationary, time– frequency analysis methods, particularly wavelet-based techniques, are employed to capture transient features that are not easily observable in the time domain alone. These processed signals are subsequently converted into structured representations, such as image- like formats, to facilitate their use in machine learning models. Where available, experimentally acquired vibration data may also be incorporated to enhance the reliability and generalization of the approach.

For feature learning, advanced data-driven methods are adopted to automatically extract meaningful patterns from the processed inputs. Convolutional neural network-based models are selected due to their effectiveness in handling complex signal and image data. These models are refined through fine- tuning and parameter optimization to better suit the characteristics of the bearing dataset. The learned feature representations are then supplied to a classification stage, where multiple algorithms are assessed to identify the most accurate and stable model for fault identification.

In the final stage, the trained system classifies the bearing condition into predefined categories, including normal operation, inner race defect, outer race defect, and rolling element fault. The effectiveness of the proposed methodology is evaluated using standard performance metrics such as accuracy, precision, recall, and F1-score. By integrating physics-based simulation with intelligent learning techniques, this approach offers a comprehensive and reliable solution for bearing fault diagnosis.

2.1. Experimental setup and data acquisition: The experimental framework in this work is developed to record vibration responses from a bearing system under varying health conditions. A laboratory-scale rotating machinery setup fitted with rolling element bearings is employed to emulate practical operating environments. Vibration signals

are captured using accelerometers mounted on the bearing housing, ensuring direct measurement of mechanical responses. The data acquisition unit is configured with a sufficiently high sampling rate to preserve important frequency components related to potential faults. Data is collected across different conditions, including healthy operation as well as defective states such as inner race, outer race, and ball faults, to ensure a diverse and representative dataset. The collected vibration signals serve as the initial input to the proposed diagnostic pipeline.

Due to the presence of noise and non-relevant variations in raw measurements, a pre-processing stage is applied to improve data quality. In this phase, wavelet- based analysis is used to break down the signals into time– frequency representations, making it easier to capture localized and transient fault signatures. These processed signals are then transformed into image-like formats, such as scalograms or similar representations, which are more suitable for analysis using deep learning techniques.

The resulting dataset comprises labelled vibration images corresponding to different bearing conditions. This dataset is systematically divided into training and testing subsets to enable reliable model development and evaluation. The training data is used to learn distinguishing features of each condition, while the testing data is reserved for performance validation. This well-organized experimental and data acquisition procedure provides a strong foundation for building an accurate and dependable bearing fault diagnosis system

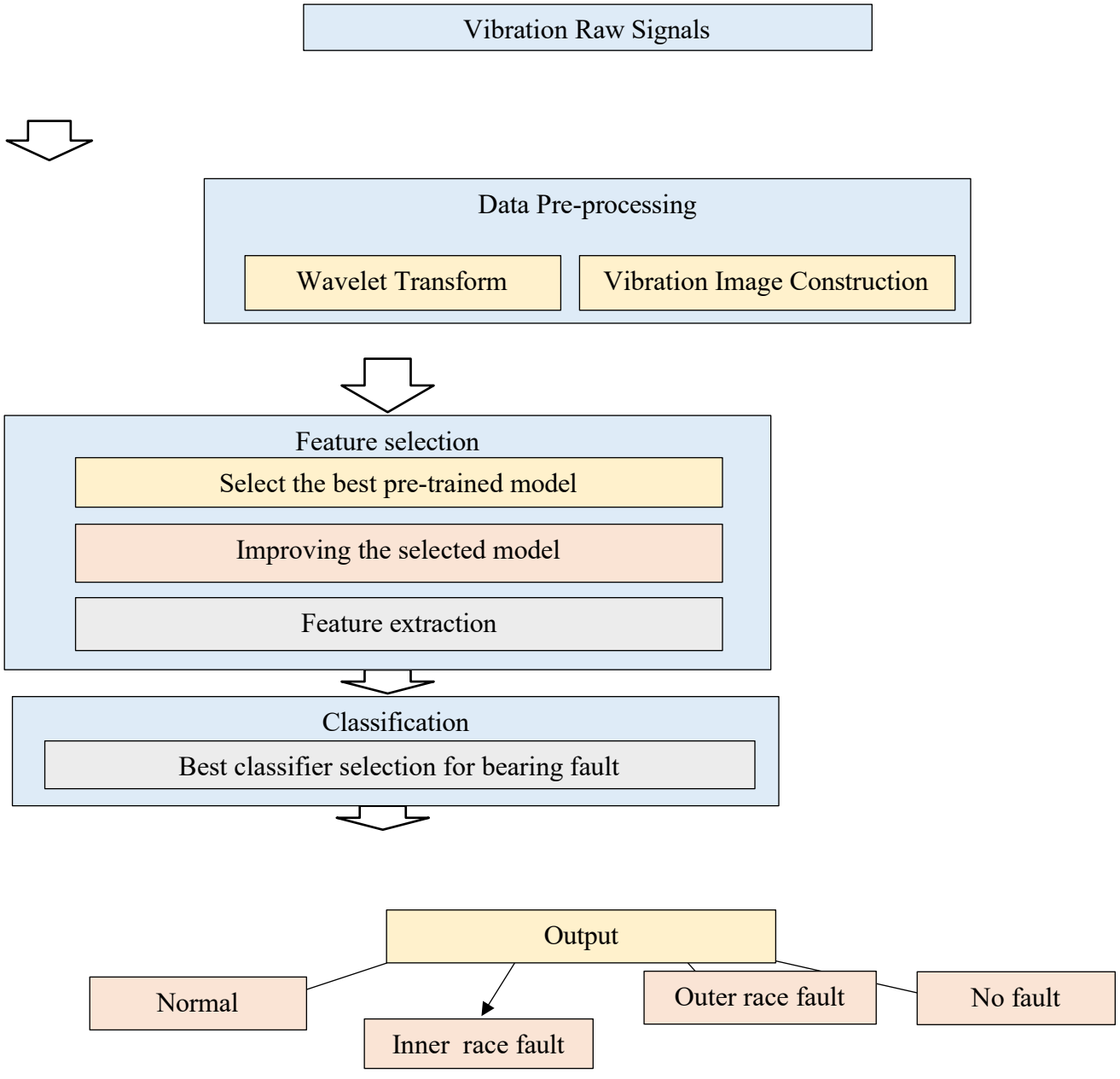

Fig 2. Methodology Of Flowchart

Table 2. Bearing defect dimension.

Sr. No.	Position of defect	Size of fault (mm)	Defect geometry
1	1 (diameter) x 1 (depth)	Circular	
2	Roller	1.5 (width) x 1.5 (length) x 1.5 (depth)	Square
3	2 (width) x 7 (length) x 2 (depth)	Line	

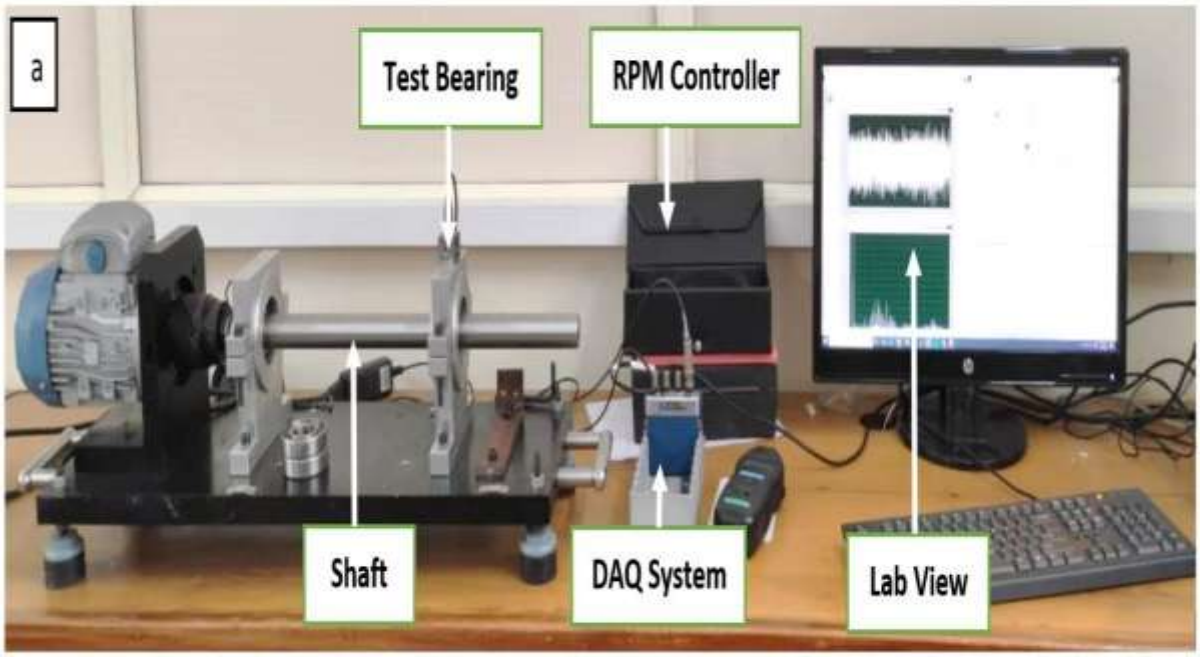

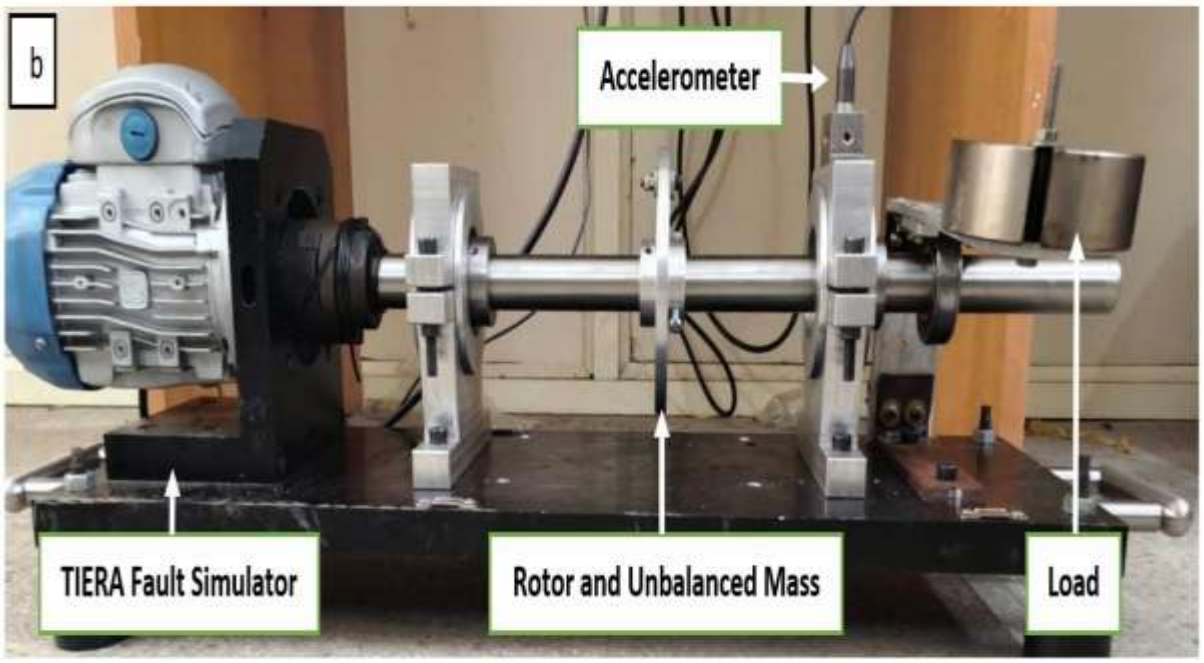

Fig. 3. Test setup: (a) healthy condition; (b) condition with artificial faults and unbalanced (c) schematic diagram of experimental test setup.

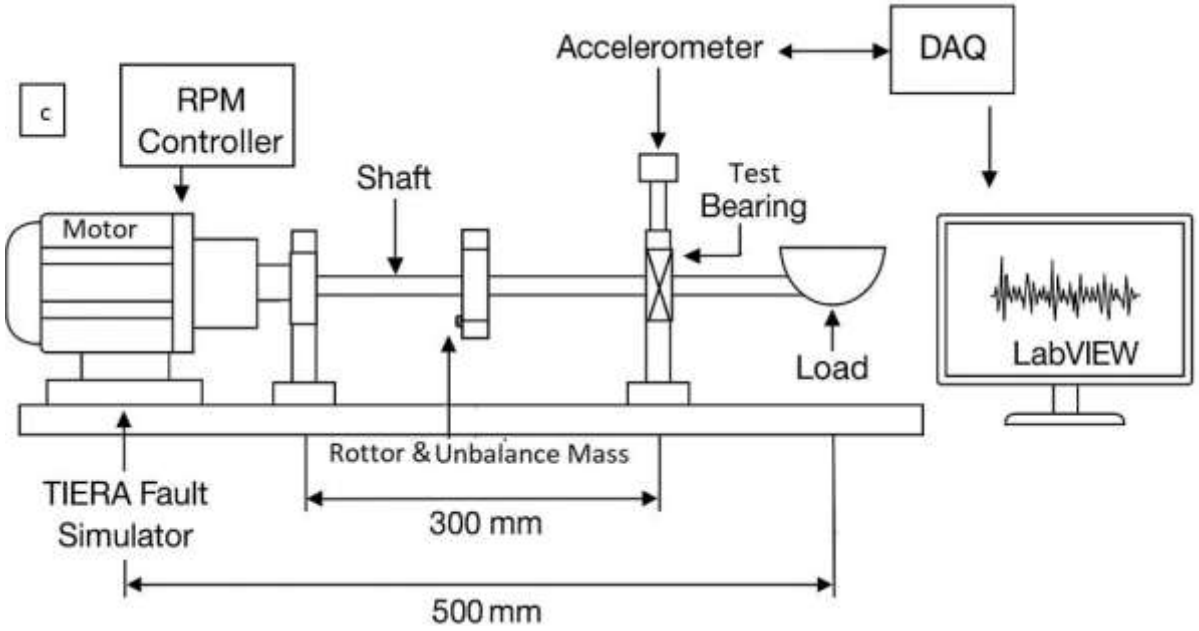

2.2. Feature extraction:

Vibration signals from machinery, particularly rolling element bearings, can be effectively analyzed using time-domain techniques to identify potential faults. This approach is considered straight forward and practical because it works directly with the raw vibration signal over time. From these signals, several statistical indicators can be derived, including root mean square (RMS), crest factor, and kurtosis. Among these, kurtosis stands out as a highly sensitive parameter because it reflects how sharply peaked or impulsive a signal is. In real-world applications, an increase in kurtosis often signals irregular impacts or shocks within the system, which are commonly linked to developing defects in bearing components.

From a mathematical perspective, kurtosis is calculated using the fourth central moment of the signal, divided by the standard deviation raised to the fourth power. This formulation ensures that the value is normalized and not affected by the overall magnitude of the signal. Essentially, it measures how much the signal deviates from its average pattern in terms of extreme values. Under normal operating conditions, vibration signals tend to be relatively smooth and evenly distributed, resulting in lower kurtosis values. However, when damage such as pitting, cracks, or surface wear occurs, it produces sudden spikes in vibration amplitude. These sharp transients significantly increase the kurtosis value, making it a reliable indicator for early fault detection in condition monitoring systems.

[1] $$K = \frac{\sum_{i=1}^{N}(y_i - \bar{y})^4}{N * \sigma^4}$$

To further investigate these effects, an experimental study was conducted under varying operational conditions. Bearings were tested at different rotational speeds 1000, 1500, and 2000 revolutions per minute and subjected to different load levels, such as 2 kg and 3 kg. Faults were deliberately introduced into the inner race of the bearings in different forms, including circular, square, and linear defects. In addition, imbalance conditions were simulated by adding small masses of 10 g, 15 g, and 20 g to the rotating system. By systematically varying these parameters, the study aimed to observe how vibration responses change with different fault types and operating scenarios, providing deeper insight into the relationship between signal characteristics and mechanical health. Additionally, combining multiple time-domain features such as RMS, crest factor, and kurtosis improves the accuracy of fault detection in rolling element bearings. While RMS reflects the overall vibration energy and crest factor highlights sudden peaks, kurtosis captures impulsive behaviour caused by defects. Using these parameters together provides a more reliable indication of bearing condition, especially under varying speeds and loads, making the diagnostic process more robust and effective. Experimental setup and data acquisition.

2.3. Rolling element bearing defects:

Common defect types-

The most frequently observed defects in rolling element bearings (reb) include surface damage such as cracks and pitting. These defects commonly appear on the outer race, inner race, and the rolling elements themselves, as illustrated in fig. 1. Such imperfections usually develop due to repeated loading, material fatigue, inadequate lubrication, or contamination, and they can significantly affect the performance and lifespan of the bearing. Rolling element bearings are composed of two concentric rings, known as the inner raceway and outer raceway, along with a series of rolling elements that move within these raceways. As the motion of these bearings is generally periodic in nature, it becomes straightforward to determine the characteristic defect frequencies associated with faults in different bearing components.

In a rolling element bearing, the rolling elements are held in position by a cage, which maintains equal spacing between them and avoids direct contact. The motion of the bearing components can be explained through five fundamental types of movement: the rotational frequency of the shaft, the cage (or fundamental train frequency), the ball pass frequency of the inner race, the ball pass frequency of the outer race, and the rotational frequency of the rolling elements. Each of these motions is associated with a specific characteristic frequency that helps in analyzing bearing behavior and detecting faults.

The five fundamental motions of a rolling element bearing, along with their respective frequencies, are illustrated in fig. 2. Among these, certain characteristic frequencies are particularly important for condition monitoring and fault diagnosis, as they indicate defects associated with specific bearing components.

(a) Shaft rotational frequency (Fs): In a bearing-rotor system, the shaft rotational frequency (Fs) represents the speed at which the shaft rotates. It is considered the primary motion in the bearing system, as all other characteristic frequencies are dependent on this fundamental rotational speed.

(b) Fundamental cage frequency (Fc): The fundamental cage frequency (Fc) refers to the rotational speed of the bearing cage. This frequency is determined based on the average linear velocities of the inner and outer raceways, since the cage moves in relation to both surfaces.

(c) Ball pass raceway frequencies (F_{BPO} and F_{BPI}): Ball pass frequencies indicate how often the rolling elements pass over specific points on the raceways. F_{BPO} (ball pass outer raceway frequency) corresponds to the frequency at which balls pass over a point on the outer raceway, while F_{BPI} (ball pass inner raceway frequency) represents the same for the inner raceway. These frequencies depend on factors such as the number of rolling elements, shaft rotational speed, and cage frequency.

(d) Ball Pass Frequency of Rolling Element (Fb): The ball pass frequency of a rolling element (Fb) represents the rate at which a specific point or defect on a ball comes into contact with the inner and outer raceways during rotation. This frequency depends on several parameters, including the number of rolling elements, the shaft rotational speed, and the geometrical properties of the bearing such as ball diameter and pitch diameter.

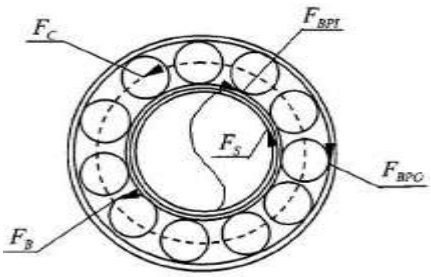

Fig 2. Frequency of four basic motions of bearing

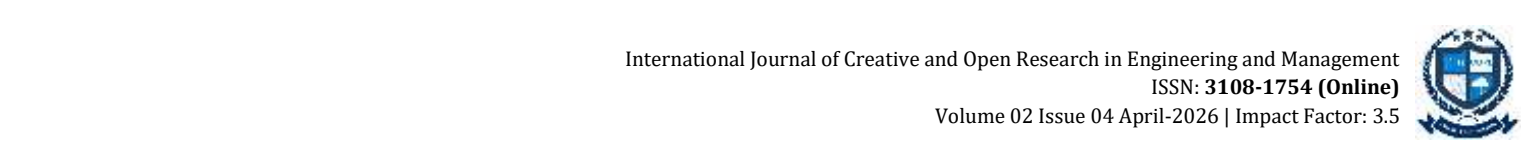

Results Geometry

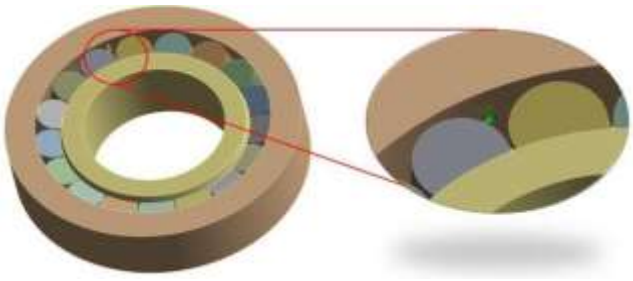

With Circular Defect

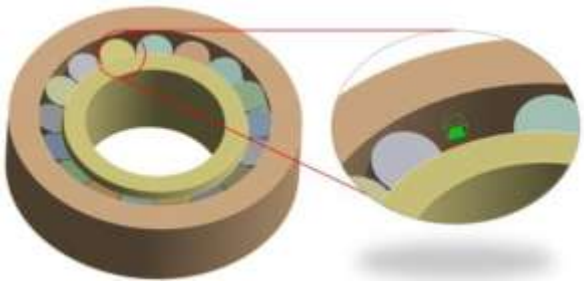

With Square Defect

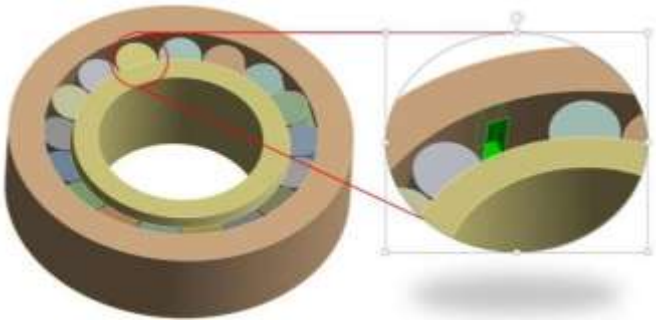

With Line Defect

In this work, detailed three-dimensional models of tapered roller bearings (30205, 30206, and 30207) were constructed using ANSYS Workbench to replicate practical operating conditions. The geometrical configurations of the bearings, including the inner race, outer race, and rolling elements, were developed based on standard design parameters. To simulate fault conditions, controlled material removal was performed on the raceway surfaces to introduce artificial defects. Three distinct defect shapes—circular, square, and linear—were incorporated to represent typical damage mechanisms such as surface pitting, localized deformation, and spall formation. The size and location of these features were selected in accordance with the experimental design to ensure consistency between numerical modelling and physical testing. This modelling strategy enables systematic evaluation of how different defect geometries influence vibration behaviour and fault signatures, thereby supporting further analysis for condition monitoring and intelligent fault diagnosis.

Boundary condition

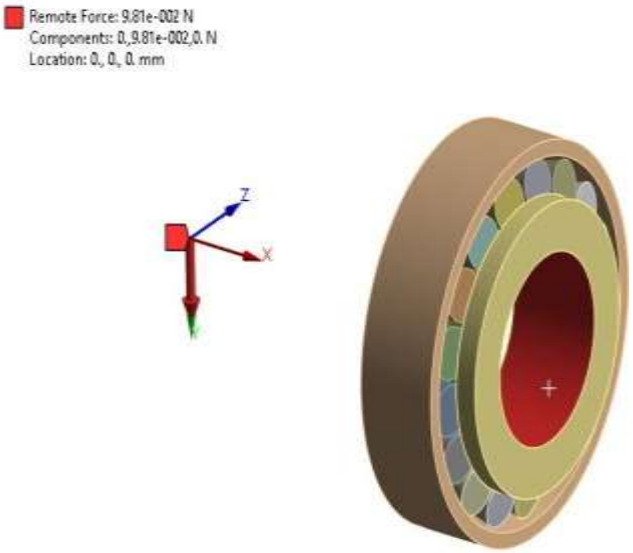

In the present finite element analysis, appropriate boundary conditions were defined to replicate the actual operating behaviour of tapered roller bearings (30205, 30206, and 30207). The outer race was constrained using a fixed support to represent its rigid connection with the housing. A revolute joint was applied to the inner race, allowing rotation about the central axis while restricting all other degrees of freedom. Rotational speeds of 1000, 1500, and 2000 rpm were imposed on the inner race to simulate different operating conditions. To represent loading conditions, radial loads of 1 kg, 2 kg, and 3 kg (equivalent to 9.81 n, 19.62 n, and 29.43 n) were applied in the y-direction on the inner race surface, corresponding to the primary load acting during operation. In addition, rotor imbalance effects were incorporated by introducing unbalanced masses of 0 g, 10 g, 15 g, and 20 g through a remote point located at the shaft center. The resulting centrifugal forces generated due to this imbalance were transmitted to the inner race. These boundary conditions collectively provide a realistic representation of operating conditions and facilitate accurate analysis of vibration response and defect-related behaviour.

Results –B30205

Defect type	**Rotational velocity (RPM)**	**Bearing Load (kg)**	**Unbalanced mass (g)**	**Theoretical Freq (Hz)**	**Peak Acceleration in (Y) (m/s^2)**	**Time at Peak acceleration (s)**	**Simulation Freq (Hz)**
Circular	1000	1	10	119.034	0.0470	0.00823	121.5067
Circular	1000	1	15	119.034	0.0489	0.00818	122.2494
Circular	1000	1	20	119.034	0.0497	0.0080	125
Square	1500	2	10	178.551	0.0916	0.00557	179.5332
Square	1500	2	15	178.551	0.0946	0.00554	180.5054
Square	1500	2	20	178.551	0.0956	0.00551	181.4882
Line	2000	3	10	238.068	0.1527	0.00418	239.23

Line	2000	3	15	238.068	0.1645	0.00417	239.80
Line	2000	3	20	238.068	0.1775	0.00414	241.54

The table presents the outcomes of a finite element study performed on a tapered roller bearing (30205) to evaluate the influence of defect geometry and operating conditions on vibration response. Three types of defects—circular, square, and line—were introduced on the bearing surface and analyzed at rotational speeds of 1000, 1500, and 2000 RPM. The analysis was conducted under varying loads of 1 kg, 2 kg, and 3 kg, along with unbalanced masses of 10 g, 15 g, and 20 g, to simulate realistic operating environments and assess system behavior.

A comparison between theoretical and simulated frequencies is presented in the table. The theoretical frequencies were determined using analytical expressions based on bearing kinematics and rotational speed, whereas the simulated frequencies were obtained from the acceleration response in the Y and Z directions, with the X-axis aligned along the shaft. The time corresponding to peak acceleration was used to estimate the associated frequency. The close agreement between analytical and simulated results confirms the reliability and accuracy of the developed model.

The table also includes peak acceleration values to represent the intensity of vibration under different conditions. It is observed that the peak acceleration increases with rising rotational speed, applied load, and unbalance magnitude. Furthermore, the defect geometry significantly affects the vibration response. Among the considered cases, line defects generate the highest acceleration levels, followed by square defects, while circular defects result in comparatively lower values. This behavior can be attributed to the presence of sharp edges in line and square defects, which induce higher stress concentrations and more severe impact forces during operation.

Results –B30205-Line defect-2000RPM-3Kg bearing Load-20g of unbalance

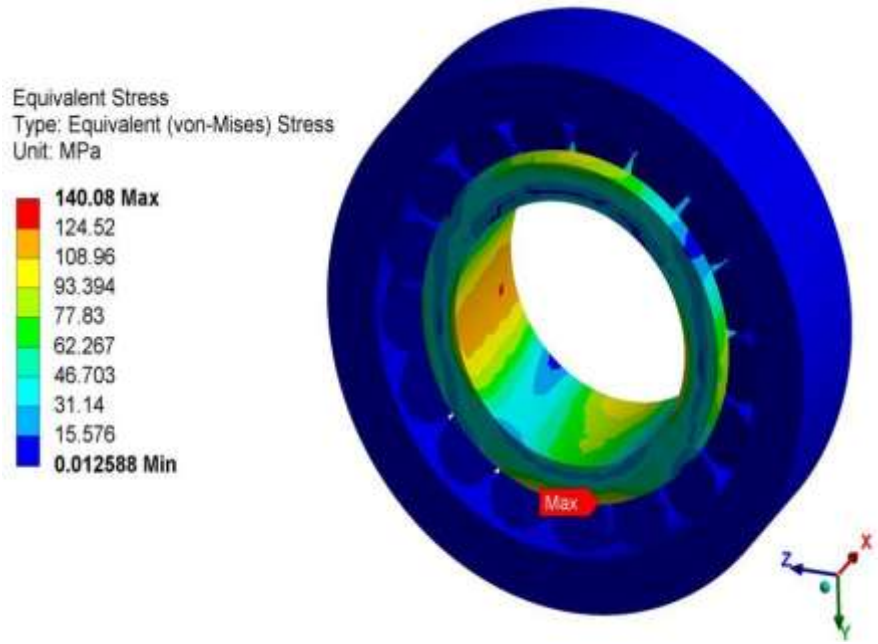

Equivalent Stress (Mpa)

The figure illustrates the finite element results for a tapered roller bearing (30205) containing a line defect, operating at 2000 RPM under a radial load of 3 kg and an unbalance of 20 g. The distribution of von Mises stress is presented to

evaluate the combined stress state and identify regions susceptible to material failure. A color contour is used to represent stress variation, where dark blue corresponds to minimum stress levels (approximately 0.012 mpa) and red indicates maximum stress values (around 140 mpa), providing a clear visualization of stress distribution across the bearing components.

It can be observed that the maximum stress is concentrated near the inner race, particularly at the defect location. These high-stress regions are depicted in red and orange, indicating severe localized loading. This behavior is primarily due to the presence of the line defect, which disrupts the continuity of the raceway surface and leads to significant stress concentration. During operation, the rolling elements repeatedly pass over the region, generating cyclic contact forces. The combined effect of rotational motion, applied radial load, and unbalance further amplifies these localized stresses, resulting in non-uniform load distribution.

In contrast, the outer regions of the bearing exhibit relatively lower stress levels, as indicated by blue and green contours. These area are less influenced by the defect and experience more uniform load transfer. The gradual transition in color from low to high stress regions reflects the path of load transmission from the rolling elements to the raceways.

Overall, the results highlight that line defects significantly increase localized stress, which may accelerate fatigue damage and crack initiation over time. Such analysis is valuable for identifying critical stress zones, enhancing bearing design, and supporting predictive maintenance strategies to prevent premature failure.

Results –B30206

Defect Type	**Rotational velocity RPM**	**Bearing Load (kg)**	**Unbalance Of mass (g)**	**Theoretical Freq (Hz)**	**Peak Acceleration in (Y) (m/s²)**	**Time at Peak acceleration in (s)**	**Simulation Freq (Hz)**
Circular	2000	2	10	237.023	0.113	0.00412	242.7184
Circular	2000	2	15	237.023	0.115	0.00411	243.309
Circular	2000	2	20	237.023	0.119	0.00410	243.9024
Square	1000	3	10	118.803	0.138	0.00850	117.6471
Square	1000	3	15	118.803	0.155	0.00849	117.7856
Square	1000	3	20	118.803	0.159	0.00841	118.9061
Line	1500	1	10	177.767	0.245	0.00566	176.6784
Line	1500	1	15	177.767	0.275	0.00569	175.7469
Line	**1500**	**1**	**20**	**177.767**	**0.276**	**0.00571**	**175.1313**

In the finite element analysis, the bearing model is discretized into a large number of small elements to accurately capture the influence of defects on vibration behavior. The key parameters evaluated include theoretical frequency, simulated frequency, peak acceleration, and the corresponding time at which peak acceleration occurs. For the circular defect at 2000 RPM under a 2 kg load, the analytical frequency (237.023 Hz) shows good agreement with the simulated range (242.71–243.90 Hz). A gradual increase in peak acceleration is observed, rising from 0.113 m/s² to 0.119 m/s² as the unbalanced mass increases. In the case of the square defect at 1000

RPM and 3 kg load, the theoretical frequency (118.803 Hz) closely matches the simulated values (117.64–118.90 Hz). However, higher vibration levels (0.138–0.159 m/s²) are recorded compared to the circular defect, which can be attributed to stress concentration at the sharp corners of the defect geometry. For the line defect at 1500 RPM with a 1 kg load, the most significant vibration response is observed. The peak acceleration increases from 0.245 m/s² to 0.286 m/s², while the simulated frequencies (175.13–176.57 Hz) remain close to the theoretical value (177.767 Hz). Overall, the results demonstrate that vibration characteristics are strongly influenced by defect geometry, rotational speed, applied load, and unbalance. Among the defect types, the line defect produces the most severe dynamic response. Furthermore, the close correspondence between theoretical and simulated frequencies validates the accuracy and reliability of the developed finite element model.

Results –B30206-Line defect-1500RPM-1Kg bearing Load-20g of unbalance Equivalent Stress (Mpa)

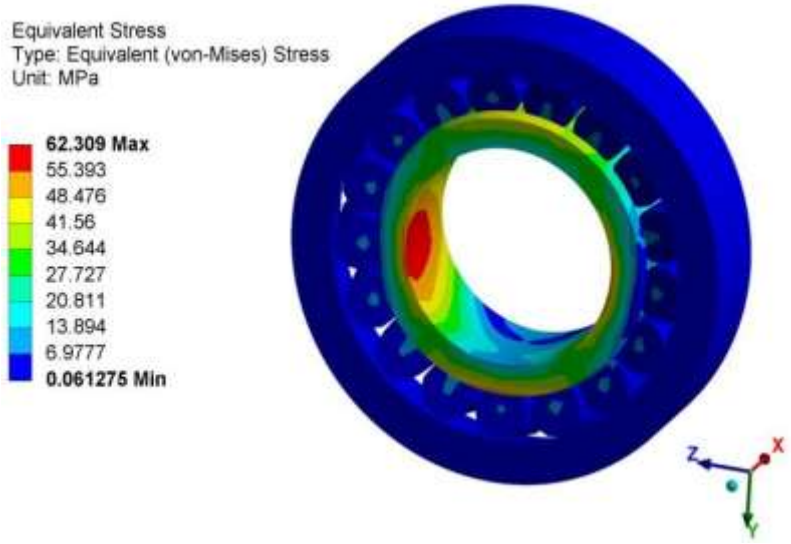

The Fig. shows the FEA result of a B30206 bearing with a line defect operating at 1500 RPM under a 1 kg load and 20 g unbalance. In FEA, the bearing is divided into small elements to calculate stress at different points. The plot represents von Mises stress, which helps identify regions that may fail under combined loading. The color scale ranges from about 0.061 MPa (blue) to 62.309 MPa (red). Most areas are blue, indicating low stress, while regions near the defect show higher stress in green to red colors. The maximum stress occurs near the inner raceway due to the defect, which acts as a stress concentration point. Because of rotation and unbalance, the load is uneven, causing higher stress where the rolling elements interact with the defect. The stress gradually decreases away from this region. This analysis helps locate critical zones where cracks or failure may start, making it useful for design improvement and maintenance planning.

Results –B30207

Defect Type	Rotational velocity RPM	Bearing Load (kg)	Unbalance (g)	Theoretical Freq (Hz)	Peak Acceleration in (Y) (m/s²)	Time at Peak Acceleration (s)	Simulation Freq (Hz)
Circular	1500	3	10	178.205	0.146	0.00561	178.2531
Circular	1500	3	15	178.205	0.149	0.00562	177.9359
Circular	**1500**	**3**	**20**	**178.205**	**0.151**	**0.00563**	**177.6199**
Square	2000	1	10	237.607	0.103	0.00421	237.5297
Square	2000	1	15	237.607	0.105	0.00424	235.8491
Square	2000	1	20	237.607	0.107	0.00429	233.1002
Line	1000	2	10	118.803	0.00951	0.00842	118.7648
Line	1000	2	15	118.803	0.00952	0.00846	118.2033
Line	1000	2	20	118.803	0.00955	0.00849	117.7856

The Table shows the results of a finite element analysis (FEA) carried out on a B30207 bearing to understand how different defect shapes influence its vibration response. The bearing is broken into small elements so that changes in stress and motion can be studied in detail, especially around the defect area. The table lists conditions such as speed, load, and unbalanced mass, along with theoretical and simulated frequencies, peak acceleration, and the time at which peak acceleration occurs. For the circular defect at 1500 RPM and 3 kg load, the frequency is close to 178 Hz, and the peak acceleration increases slightly as unbalance increases from 10 g to 20 g, indicating higher vibration levels. In the square defect case at 2000 RPM and 1 kg load, the frequency rises to about 237 Hz due to higher speed, while the acceleration values remain moderate but increase gradually with unbalance. For the line defect at 1000 RPM and 2 kg load, the frequency is around 118 Hz, and the acceleration is much lower, showing weaker vibrations. The time at peak acceleration is nearly the same in all cases, indicating steady behaviour. Acceleration is measured along the Y and Z directions, and frequency is obtained from the time response. Overall, the results show that speed mainly affects frequency, unbalance affects vibration level, and defect shape controls how severe the response is, with simulated values closely matching theoretical results.

Results –B30207-circulardefect-1500RPM-3Kg bearing Load-20g of unbalance Equivalent Stress (Mpa)

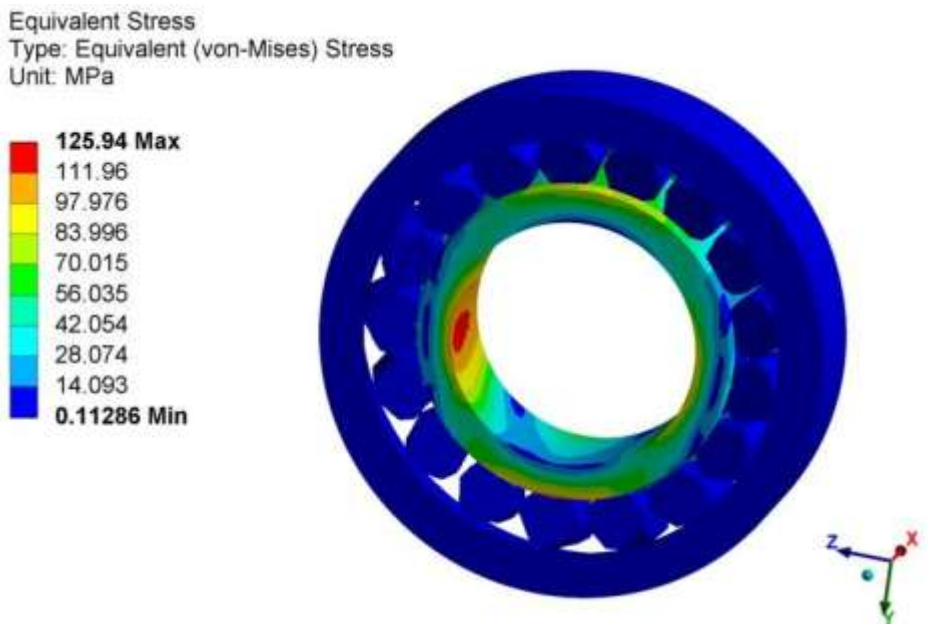

The figure illustrates the distribution of equivalent (von Mises) stress within a tapered roller bearing under defined operating conditions. The stress values vary from approximately 0.112 MPa (represented by dark blue) to a peak value of 125.94 MPa (represented by red), clearly showing how stress is distributed across different types of the bearing. The highest stress levels are concentrated along the inner raceway, particularly in the contact region between the rolling elements and the race surface. These regions, highlighted in red and orange, indicate zones subjected to intense localized loading. This concentration occurs due to repeated contact forces during rotation, which become more pronounced in the presence of defects or surface discontinuities that disrupt uniform load sharing. Areas surrounding the high-stress zones show moderate stress levels, depicted in green and yellow, indicating gradual transfer of load through the rolling elements and raceways. In contrast, the outer race and other regions exhibit comparatively lower stress levels, as indicated by blue shades, suggesting more uniform and stable loading conditions. The gradual variation in color from low to high stress demonstrates the path of load transmission within the bearing. Overall, the results emphasize that localized stress concentrations, especially near defective regions, can accelerate fatigue damage and initiate crack formation. Such analysis is important for identifying critical zones, optimizing bearing design, and planning effective maintenance strategies to prevent failure.

Time domain and frequency domain analysis:

Table1: Characteristic frequencies of rolling element bearing defects with corresponding formulas:

Characteristics Frequencies	**Formula**
Inner race defect frequency (BPFI) Hz	$\frac{nf_r}{2}\left\{1+\frac{d}{d}\cos\emptyset\right\}$
Outer race defect frequency (BPFO) Hz	$\frac{nf_r}{2}\left\{1-\frac{d}{d}\cos\emptyset\right\}$
Cage frequency (FTF) Hz	$\frac{f_r}{2}\left\{1-\frac{d}{d}\cos\emptyset\right\}$

Rolling element spin frequency (RSF) Hz	$\frac{df_r}{2d}\left\{1-\left(\frac{d}{d}\cos\emptyset\right)^2\right\}$
Rolling element defect frequency (RDF) Hz	$\frac{df_r}{d}\left\{1-\left(\frac{d}{d}\cos\emptyset\right)^2\right\}$

The "Formula" Column provides the corresponding mathematical formulas for calculating each of these characteristic frequencies. These formulas involve variables such as the number of rolling elements (n), the diameter of the rolling elements (d), the diameter of the bearing (d), the rotational frequency (fr), and the contact angle (θ).

Table 2: Defect Frequency For Skf 30205, Skf 302056 & Skf 30207.

Bearing	**Speed (rpm)**	**Speed (hz)**	**BPFI**	**BPFO**	**FTF**	**BSF**	**RDF**
30205	1000	16.667	164.2991	119.0342	7.002011	49.31305	98.62611
	1500	25	246.4487	178.5513	10.50302	73.96958	147.9392
	2000	33.33	328.5983	238.0684	14.00402	98.62611	197.2522
30206	1000	16.667	164.8218	118.5115	6.971266	48.14096	96.28193
	1500	25	247.2327	177.7673	10.4569	72.21145	144.4229
	2000	33.33	329.6436	237.0230	13.94253	96.28193	192.5639
30207	1000	16.667	164.5300	118.8033	6.98843	48.78888	97.57777
	1500	25	246.7950	178.2050	10.48265	73.18333	146.3667
	2000	33.33	329.0600	237.6066	13.97686	97.57777	195.1555

Characteristic frequencies such as BPFI, BPFO, FTF, RSF, and RDF serve as essential indicators in the analysis of vibration signals from rotating machinery bearings. These frequencies are utilized in both time-domain and frequency-domain methodologies for diagnosing the presence and location of faults within a bearing. In advanced

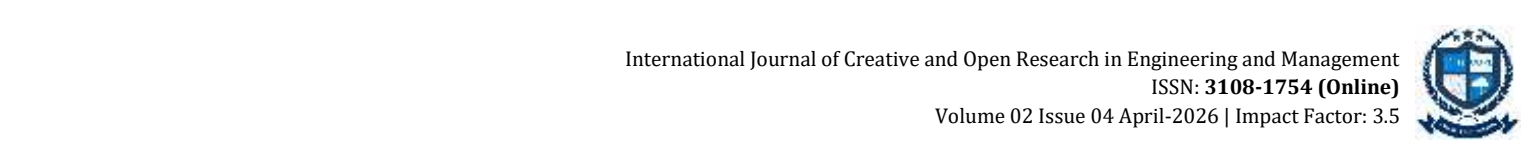

diagnostic applications, including those that employ artificial neural networks or other machine learning strategies, these characteristic frequencies become key features for classification and detection tasks.by comparing the calculated characteristic frequencies—with exact values derived from bearing geometry and operating conditions—to the prominent peaks observed in the vibration spectrum, engineers and automated systems can pinpoint the specific type and position of a defect, such as damage on the inner race, outer race, rolling elements, or cage. The accuracy of this approach relies heavily on having correct details about the bearing's dimensions and rotational parameters, as errors in this data can directly affect fault identification

Experimental readings consistently displayed defect signatures, with strong harmonics appearing at multiples of the fault frequency, which reinforced the presence of bearing defects. These distinct frequency-domain features, such as harmonics and side bands, enable precise isolation and monitoring of fault patterns across various operational scenarios. Importance of frequency-domain analysis frequency domain analysis plays a crucial role in bearing condition monitoring by decomposing vibration signals into their specific frequency components. This approach filters out noise and highlights fault-related frequencies and their harmonics, providing clearer visualization and facilitating early detection of characteristic bearing faults. The spectral patterns associated with specific defects allow quick differentiation between faulty and normal bearings even in noisy environments. Consistency in defect patterns across different experimental tests, the remaining data sets showed similar fault- related patterns, further validating the diagnostic reliability of frequency domain techniques in identifying bearing defects and their harmonics. Evaluating frequencies and amplitudes within the spectrum provides repeatable evidence of bearing faults, making this method essential for effective condition monitoring and maintenance. The noticeable presence of higher-order harmonics at multiples of the fault frequency confirmed the existence of a bearing defect. This observation highlights the value of frequency-domain analysis in accurately detecting defect- related frequency components and their harmonics for reliable condition monitoring, as depicted in fig 3 & 4. The other experimental results exhibited comparable fault characteristics, reinforcing the consistency and dependability of the proposed fault diagnosis method based on both time-domain and frequency-domain analysis under varying operating conditions and bearing types

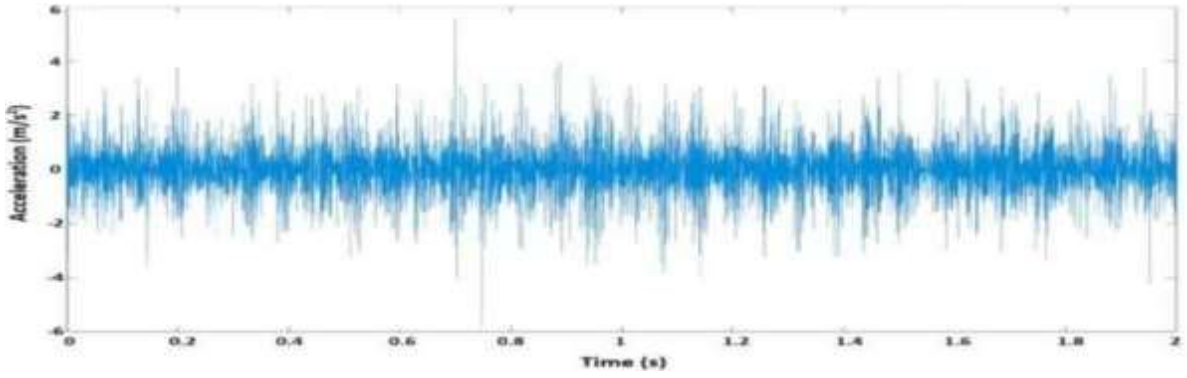

(a)

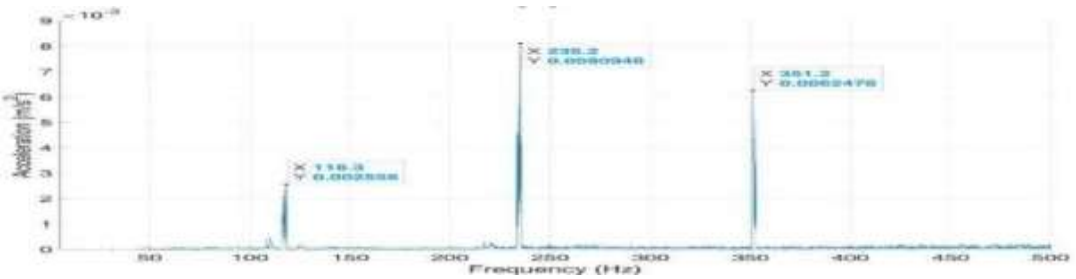

(b)

Fig 3 Vibration Signals For 30205J2/Q Healthy Bearing At 1000 RPM a) Time Domain b) Frequency Domain.

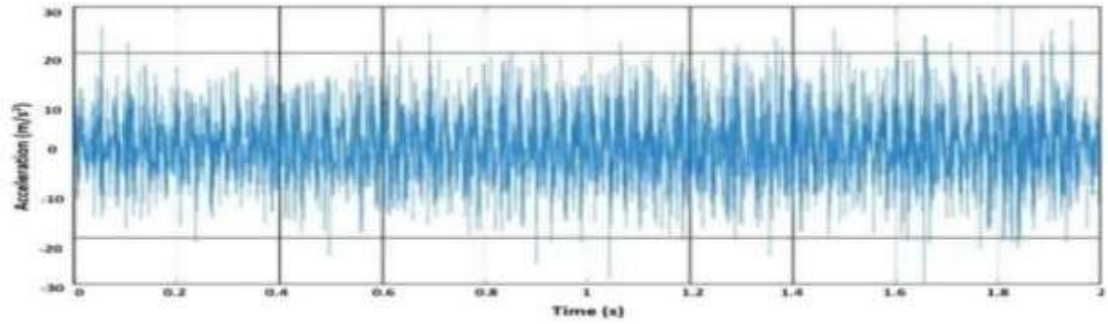

(a)

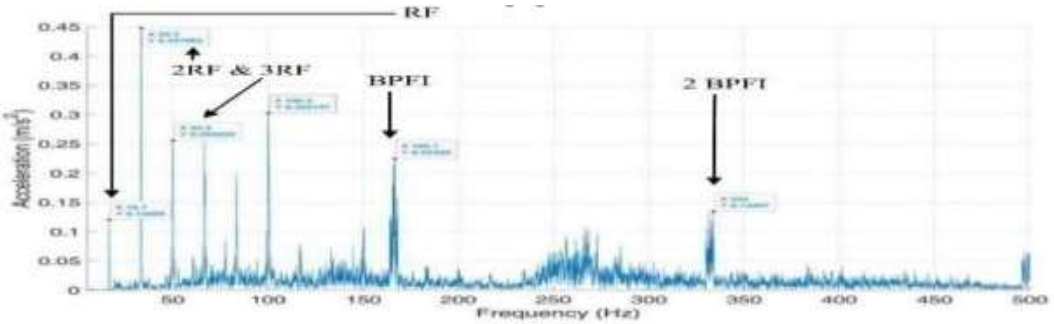

(b)

Fig 4 Vibration Signals 30205J2/Q Bearing And Inner Race Defect Condition (Load 1 Kg, circular defect 1000 RPM and 10g unbalance)

Reference:

[1] H. Aher, N. Ghuge, Vibration-based condition monitoring of tapered roller bearings using kurtosis and ANOVA, Tribology in industry 47 (2) (2025), https://doi.org/ 10.24874/ti.1934.04.25.06.

[2] H.R. Aher, N.C. Ghuge, Performance comparison of machine learning algorithms for condition monitoring of tapered roller bearings, Tribology and materials. 4 (2) (2025) 100–115, https://doi.org/10.46793/tribomat.2025.009.

[3] Y. Zhang, H. Zuo, F. Bai, Classification of fault location and performance degradation of a roller bearing, Measurement 46 (3) (2013) 1178–1189, https:// doi.org/10.1016/j.measurement.2012.11.025.

[4] Li, Q., Ning, J., Liang, H. & Yang, M. (2025). High-Speed Bearing Reliability: Analysis of Tapered Roller Bearing Performance and Cage Fracture Mechanisms. Metals, 15(6), 592. https://doi.org/10.3390/met15060592

[5] Y. Dong, Y. Ma, M. Qiu, F. Chen, and K. He, "Transient temperature rise in high-speed cylindrical roller bearings of a spindle system: A hybrid thermal-structural prediction approach with real-time validation," Mechanical Systems and Signal Processing, 2024.

[6] Saadi Laribi, S., Bendiabdellah, A., & Meradi, S. (2020). Condition monitoring improvement of rolling element bearings using multilayer perceptron artificial neural network based on time-domain vibration features. Journal of Electrical Systems, 16(3), 450–462.

[7] Shaik, M. R., & Mulpur, S. B. (2016). Fatigue life, modal vibration, and transient dynamic analysis of a tapered roller bearing using finite element method. International Journal of Engineering Research & Technology (IJERT), 5(3), 611–616.

[8] U. Igie and T. Sibilli, "Transient thermal modelling of ball bearing using finite element method," J. Eng. Gas Turbines Power, vol. 140, no. 3, 2018, Art. no. GTP-16-1232, doi:10.1115/1.4037861.

[9] B. Samanta and K. R. Al-Balushi, "Artificial neural network based fault diagnostics of rolling element bearings using time-domain features," Mechanical Systems and Signal Processing, vol. 15, no. 2, pp. 307–318, 2001.

[10] S. Tyagi and S. K. Panigrahi, "Finite-element modeling and analysis of transient dynamic behavior of ball bearings with localized faults," Journal of Sound and Vibration, vol. 333, no. 7, pp. 2079–2093, 2014.

[11] Zhang et al., "Bridging the simulation-to-reality gap for bearing fault diagnosis using high fidelity vibration simulations and transfer learning," Mechanical Systems and Signal Processing, 2025.